Astron. Astrophys. 335, 807–822 (1998)

ASTRONOMY AND ASTROPHYSICS

Resolved 200μm images of nearby galaxies – evidence for an extended distribution of cold dust*

P.B. Alton[1], M. Trewhella[2], J.I. Davies[1], R. Evans[3], S. Bianchi[1], W. Gear[4], H. Thronson[5], E. Valentijn[6], and A. Witt[7]

[1] Department of Physics & Astronomy, University of Wales, P.O. Box 913, Cardiff CF2 3YB, UK
[2] Infrared Processing and Analysis Center, Caltech, M.S. 100-22, Pasadena CA 91125, USA
[3] University of Chicago Yerkes Observatory, 373, West Geneva St., Williams Bay, WI 53191, USA
[4] Mullard Space Science Laboratory, University College London, Holmbury, Surrey RH5 6NT, UK
[5] Code SR, NASA Headquarters, 300 E.Street SW, Washington DC 20546, USA
[6] Kapteyn Institute, SRON, P.O. Box 800, 9700 Groningen, The Netherlands
[7] Department of Physics and Astronomy, The University of Toledo, 2801 W.Bancroft, Toledo, OH 43606, USA

Received 13 February 1998 / Accepted 15 April 1998

Abstract. We present resolved 200μm images for 8 nearby galaxies observed with the Infrared Space Observatory (ISO). By comparing the 200μm observations with IRAS 60μm and 100μm data, we find that cold dust becomes more dominant at larger radii. We infer a grain temperature of 18–21 K for this cold component i.e. about 10 K lower than the warm dust detected by IRAS in external spirals. This value is close to theoretical predictions in the literature based on heating by the general interstellar radiation field. A comparison of the 200μm images with complementary B-band data also shows that the cold dust is radially more extensive than the stars. The gas-to-dust ratio of external spirals, derived using IRAS fluxes, has been claimed to be about an order of magnitude higher than the value infered for the Galaxy. By analysing the 200μm data for our sample, we derive a mean gas-to-dust ratio of ~ 225 which is close to the value in the solar neighborhood (150–300). It is likely that IRAS may have 'overlooked' the vast majority of grains residing in spiral disks.

Key words: ISM: dust, extinction – galaxies: ISM – infrared: galaxies

1. Introduction

In this paper, we report on 200μm imaging observations of 8 nearby galaxies carried out by the Infrared Space Observatory (ISO). The ISO satellite was launched in November 1995 and is expected to operate until April 1998 yielding images and spectra of the Universe in the wavelength range 2.5–240 μm (Kessler et al. 1996). Of particular interest is the imaging photo-polarimeter, ISOPHOT, which extends the 'FIR window' to wavelengths longward of the IRAS 100μm filter. We have used the ISOPHOT P32 mapping mode to observe 8 galaxies with optical diameters (D_{25}) $\simeq 10'$. The apparent size of our selected objects ensures that they are clearly resolved by the effective beam at 200μm (FWHM $\simeq 117''$). All our targets are classified as spiral disk galaxies with the exception of one object, NGC 6822 which is a Magellanic irregular belonging to the Local Group (Gallagher et al. 1991).

The addition of 200μm data for spiral galaxies means that we are now far more likely to sample most of the energy emitted by interstellar dust grains and, indeed, locate the peak in the FIR emission curve which is expected to lie somewhere between 100 and 200 microns (Evans 1992; Disney et al (1989)). Since the energy radiated by dust grains was originally part of the optical and near-infrared flux emitted by stars, the FIR luminosity of a galaxy, as well as its distribution within the spiral disk, has direct bearing on the opacity of the disk. In fact, by collating optical, and near infrared images for a specific set of galaxies and making a comparison with the corresponding FIR emission, it is possible to infer the extinction at each point within the selected objects. Trewhella (1997) and Trewhella et al (1998) have already begun to apply this 'energy-balance' technique to the galaxies observed in this paper (see also Xu & Helou 1996) and their initial results show that interstellar dust plays an important rôle in influencing our perceptions of galaxy morphology, structure and colour. The problem of determining optical depth within spiral disks has confounded extragalactic astronomers for nearly half a century and enticed, in recent years, a diversity of observational techniques (Valentijn 1990; Disney et al (1989); Davies & Burstein (1995); Block & Greenberg (1996) and references therein). The 'energy-balance' method outlined above promises to go some way towards resolving the issue although determination of the overall transparency of spiral disks may ultimately be limited by how well we know the distribution of the dust relative to the stars (Disney et al 1989).

Another topical issue which we intend to address with our ISO observations is *how much* dust exists within spiral galaxies

Send offprint requests to: P.B. Alton, (paul.alton@astro.cf.ac.uk)

* Based on observations with ISO, an ESA project with instruments funded by ESA Member States (especially the PI countries: France, Germany, the Netherlands and the United Kingdom) and with the participation of ISAS and NASA.

and what the relevant grain temperatures are. There are already strong indications that IRAS, being primarily sensitive to grains warmer than about 30K, may have 'overlooked' quite substantial quantities of cooler dust. Indeed, silicate and graphite dust grains associated with the diffuse interstellar medium are expected to have an equilibrium temperature of only 15-20 K (Disney et al (1989); Draine & Lee (1984); Mathis et al (1983)) which would cause the FIR spectral energy distribution to peak somewhere between 150μm and 250μm for an emissivity index β = 1$\rightarrow$2 (Evans 1992).

Measurements of dust within the Galaxy have always contrasted, *prima facie*, with analogous observations carried out for external spirals. Recently, Reach et al (1995) have utilized the spectro-photometer onboard COBE (FIRAS) in order to derive the 100μm–2mm spectrum of diffuse grains within the Milky Way (see also Hauser et al (1984); Masi et al (1993)). For positions outside the Galactic plane (b$> 10^{\circ}$) they find an almost uniform dust temperature of 16–22 K – significantly colder than the 30 K grain temperature derived for external spirals using IRAS 60μm and 100μm data (Alton et al 1998a; Devereux & Young 1990). Since, for a given FIR luminosity, dust mass scales inversely as $T^{4+\beta}$ (where T and β are the dust temperature and emissivity index respectively), the seemingly higher grain temperatures recorded for external galaxies would imply rather low dust masses. Indeed, one puzzling aspect to the interstellar medium (ISM) of external galaxies has always been that their gas-to-dust ratios, derived using IRAS fluxes, appear to be about an order of magnitude higher than that of the solar neighbourhood (Devereux & Young 1990). This revelation is rather surprising given that near solar metal abundances prevail in many external galaxies (Vila-Costas & Edmunds 1992) and may persuade us that the largest fraction of dust in spiral disks has yet to be detected.

Guelin et al (1993) have carried out 1.3mm imaging observations of the nearby spiral NGC 891 using the IRAM telescope (see also Neininger et al (1996); Guelin et al (1995)). Their detection at 1.3mm is several times higher than the emission expected from a single-temperature greybody (β=2) fitted to the corresponding 60μm and 100μm IRAS fluxes. Although this conclusion is sensitive to the adopted form of the emissivity law (β=1, for example, would not result in an excess at 1.3mm), it gives an indication that large amounts of cold dust (T$\sim$ 15K) may be present in spiral disks which can only detected at submm/mm wavelengths. Using an entirely different technique, Xilouris et al (1997;1998) have recently modelled the optical and near infrared surface photometry of 2 nearby edge-on spirals by taking account of the extinction produced by the dust lane (absorption plus scattering). For both galaxies, a robust solution emerges when gas-to-dust ratios are consistent with Galactic values (150-300; Whittet 1992). In contrast, gas-to-dust ratios based on IRAS photometry of the same galaxies are an order of magnitude higher.

This paper presents 200μm images of 8 nearby galaxies. In the subsequent sections, we discuss the acquisition of our FIR data (Sect. 2), the morphological structure evident in the 200μm images (Sect. 3) and the surface brightneses at 60, 100 and 200 microns (Sect. 4). Our results, and their implications for the ISM of external galaxies, are discussed in Sect. 5.

2. Observations and reduction

2.1. ISO data

Eight galaxies (Table 1) were observed using the ISOPHOT C200 detectors in a P32 mapping mode. The objects targeted were selected on the basis of having large apparent sizes ($\sim 10'$) and, in the main, represent quiescent spiral galaxies with normal FIR-to-blue luminosity ratios (i.e. $\frac{L_{FIR}}{L_B} < 1$; Soifer et al (1987)). For all observations, a 200μm filter was used with a bandwidth of $\simeq$ 67μm (FWHM). The sampling along the in-scan and cross-scan directions was $31''$ and $93''$ respectively (for further details about the operation and behaviour of the ISOPHOT instrument see Lemke et al. 1996). Note that, for each target, a sufficiently large part of the surrounding sky was included in the mapping operation in order to allow for subtraction of the 200μm sky emission (chiefly foreground flux from Galactic cirrus). The observations were carried out between October 1996 and June 1997 and the time required to map one object was typically 40 minutes.

Reduction of the ISO data was carried out using the ISOPHOT interactive analysis software package (PIA v6.0). This corrects for non-linearity in the readout electronics and applies a deglitching algorithm to remove the effect of cosmic rays. Measurement of an internal source (the fine calibration source or 'FCS') allows the detector pixels to be flat-fielded and the signal to be converted into power (MJy/sr). The FCS measurement is carried out twice – immediately before and after mapping the object – so as to monitor any change in the detector responsivities and, if necessary, to interpolate between the two measurements.

The absolute calibration of the instrument is still subject to some uncertainty. We, therefore, carried out several checks on the photometric reliability of the data. For one of the objects in the sample, NGC 6946, Engargiola (1991) has mapped out the central $5'$ at 200μm using the Kuiper Airborne Observatory (KAO). He derived a total flux of 226$\pm$50 Jy for this region. Although our data are of poorer resolution (tending to smooth out the brightest regions of the galaxy), we obtain a somewhat higher value of 270$\pm$40 Jy over the same area. The two values are, nevertheless, consistent within the errors. We have also compared the 'sky background' recorded in the ISO map of NGC 6946 with values expected on the basis of IRAS and COBE survey measurements. Reach et al (1995) have shown, using 100μm–2mm data collected by the FIRAS instrument onboard COBE, that foreground dust at this galactic latitude is well described by a 19 K blackbody modified by a β=1.5 emissivity law. Using the 100μm 'sky' emission recorded by IRAS near NGC 6946 (15 MJy/sr), we predict, using the Reach et al spectrum, a 200μm background of 29 MJy/sr. The value we actually measure is 40 MJy/sr, which is about one third greater. A similar conclusion is drawn from examining the 200μm 'sky emission' surrounding many of the other objects in our sample, indicating that

Table 1. Galaxy sample observed by ISO. For each object, we give the following parameters: the B1950 coordinates (RA & Dec); the diameter of the major (D_{25}) and minor (d_{25}) axes out to the B-band isophote 25 mag/arcsec^2; the morphological type given by Sandage & Tammann (1981); the position angle of the ISO scan (PA); and the adopted distance based on H_0=75 kms^{-1}/Mpc (except for NGC 6822 and NGC 6946 where we use the values given by Gallagher et al (1991) and Sandage & Tammann (1974) respectively).

Galaxy	Other Names	RA (1950)	Dec. (1950)	D_{25} (arcmin)	d_{25} (arcmin)	Type	PA (deg)	Distance (Mpc)
NGC 134		00 27 54.0	-33 32 00	8.1	2.6	Sbc(s)	140	21.1
NGC 628	M74	01 34 00.6	15 31 36	10.2	9.5	Sc(s)	157	8.8
NGC 660		01 40 21.0	13 23 18	9.1	4.1	(RSa)	160	11.3
NGC 5194	M51	13 27 45.6	47 27 18	10.9	7.7	Sbc(s)	74	6.2
NGC 5236	M83	13 34 10.2	-29 36 48	11.2	10.2	SBc(s)	28	6.9
NGC 6822	D209	19 42 07.1	-14 55 42	10.2	9.5	Im	169	0.5
NGC 6946		20 33 47.9	59 59 00	10.9	9.7	Sc(s)	186	10.1
NGC 7331		22 34 47.2	34 09 30	10.7	4.0	Sb(rs)	152	10.9

Table 2. Exponential scale-lengths, measured between a radius of $1.5'$ and $3.5'$, for the 7 spiral galaxies in Table 1. For NGC 660, which is dominated by nuclear FIR emission (see text), the scale-length has been determined over the interval $1.5' \rightarrow 2.5'$.

Galaxy	60μm ($''$)	100μm ($''$)	200μm ($''$)	B ($''$)	$\frac{B}{200\mu m}$	$\frac{60\mu m}{200\mu m}$	$\frac{100\mu m}{200\mu m}$
NGC 134	47	49	83	69	0.83	0.57	0.59
NGC 628	84	71	105	81	0.77	0.80	0.68
NGC 660	29	28	94	62	0.65	0.31	0.30
NGC 5194	76	70	104	90	0.87	0.73	0.67
NGC 5236	67	79	132	127	0.96	0.51	0.60
NGC 6946	87	82	158	145	0.92	0.55	0.52
NGC 7331	47	46	86	45	0.52	0.55	0.53

the present calibration may be overestimating the flux by about 30%.

2.2. IRAS data

To compare with our ISO data, we have obtained resolution-enhanced 60μm and 100μm IRAS (HiRes) images for the galaxies in Table 1. These were obtained from the Infrared Processing and Analysis Center at Caltech (IPAC) which produces HiRes images using a maximum correlation method. This technique essentially uses modelled responses of the 62 rectangular IRAS survey detectors in order to simulate the 'observing' process as the satellite scans over the sky (Aumann, Fowler & Melnyk 1990). The simulated data are compared with the real survey data in order to correct the input image fed into the processing algorithm. This is carried out in an iterative fashion until a basic convergence is achieved between the recorded and the simulated data. In theory, restoration to the diffraction limit of the telescope is possible but in practice the amount of processing is limited by the signal-to-noise level present in the original data. The final beam is generally elliptical with the resolution along the in-scan direction somewhat closer to the diffraction limit than that along the cross-scan direction (e.g. $60'' \times 45''$ at 60μm and $100'' \times 80''$ at 100μm). In conjunction with the HiRes images we received various ancillary products including an image of the effective beam close to the observed object.

Using the information present in the HiRes beam maps we convolved the 60μm and 100μm images to the same resolution as the ISO data. From an analysis carried out by Tuffs et al. (1996), the 200μm beam is measured to be 117" at FWHM (which is somewhat broader than the theoretical Airy profile of $86''$). The convolved IRAS data were then registered with the ISO image so that the peak brightness at both wavelengths was positionally coincident. This was justified by the fact that, within positional uncertainties ($30''$), the greatest emissivity at 60μm (100μm) occurred at the same location as the maximum 200μm emission within the galaxy (usually the nucleus). The registration also involved rotating the IRAS images to the same orientation as the ISO scan and matching the pixel scale. For each galaxy in our sample, the position angle of the ISO scan is given in Table 1.

2.3. Optical images

B-band images were obtained for our galaxy sample using telescope facilities at Kitt Peak (0.9m), Skinakas observatory in Crete (1.3m), CTIO (1.5m and Curtis-Schmidt) and the Isaac Newton Telescope (2.5m). The observations were carried out during the period April 1995 to November 1997. For each observing run, the CCD frames were reduced in the standard manner (Trewhella 1997) and the final optical image rotated so that it matched the orientation of the 200μm map.

Table 3. Total flux density, at 60, 100 and 200 microns, for the 7 spiral galaxies in Table 1. In each case, the value shown represents the flux recorded within a 1σ isophote. The 60μm and 100μm flux densities are subject to an error of 10-15%, whilst the calibration of ISOPHOT probably overestimates the 200μm flux density by $\sim 30\%$ (Sect. 2.1).

Galaxy	F_{60} (Jy)	F_{100} (Jy)	F_{200} (Jy)
NGC 134	22.4	67.0	127
NGC 628	26.3	67.5	209
NGC 660	71.4	120	158
NGC 5194	130	303	533
NGC 5236	314	624	889
NGC 6946	165	338	743
NGC 7331	42.9	120	243

Table 4. Mean dust properties of the 7 spiral galaxies in Table 1. $< T >$ and $< M_d >$ denote the average grain temperature and dust mass respectively. Values are shown for calculations utilizing just IRAS data (60μm and 100μm) and for calculations which incorporate ISO data (200μm and 100μm). In the last column, we show the effect of reducing the ISO photometric calibration by 30%.

Property	β	IRAS	ISO	ISO (-30%)
$< T(K) >$	1	34	21	24
	2	28	18	19
$< M_d(M_\odot) >$	1	7.7×10^6	8.9×10^7	4.2×10^7
	2	4.3×10^6	9.5×10^7	3.2×10^7
<Gas-to-dust>	1	2800	230	494
	2	5100	220	446

3. 200μm images

In Fig. 1 we present FIR and optical images for the objects listed in Table 1. In the following paragraphs we comment briefly on the general properties of each galaxy and discuss qualitatively the FIR morphology evident in Fig. 1.

NGC 134 This is an Sbc southern galaxy inclined at an angle of about 76°. It has been included in several large surveys at various wavelengths – e.g. the FIR study of van Driel et al. (1993) and the radio continuum sample of Condon et al. (1996) – but does not appear to have been studied at an individual level. Alton et al. (1998a) found, from an analysis of the HiRes data for this object, that the 60μm emission is rather 'flat-topped' with the majority of energy arising from the inner 2–3′.

NGC 628 This galaxy, also known as M74, has been classified as type Sc and has a very small inclination to the line-of-sight (5°; Shostak & van der Kruit 1984). Like nearby M51, its grand design spiral pattern has aroused considerable interest (Cepa & Beckman 1990) and the bright HII regions pertaining to the spiral arms have also been an object of study (Kennicutt & Hodge 1980). Unusually for an isolated galaxy, NGC 628 has a very large HI disk ($> 25'$) extending well beyond the $10'$ optical diameter (Briggs et al. 1980). There is very little to suggest spiral structure in our FIR images (in contrast to, say, NGC 6946). However, this may not be surprising given that the HiRes data, before convolution to the ISO 200μm resolution, show quite a compact structure with about half of the FIR energy emanating from the central $3.5'$ of the disk.

NGC 660 This is an almost edge-on ($i = 70°$), barred spiral with quite a high FIR-to-blue luminosity ratio ($\frac{L_{FIR}}{L_B} \simeq 4$; Alton 1996, Alton et al (1998a)). It is distinguished by a massive 'polar' ring containing young stars and also copious amounts of dust and molecular gas (van Driel et al. 1996). These features, along with emission-line broadening associated with starburst-driven outflow (Armus et al. 1990), testify to a recent violent past in which NGC 660 probably collided with another galaxy. High resolution IRAS data show a bright, point-like (< 3 kpc) source associated with the nuclear starburst. In Fig. 1, the 200μm image also seems fairly 'point-like' but faint structure, possible emanating from the outer disk and polar ring, is also apparent. The compact emission at 200μm emphasizes the fact that warm dust tends to 'out-shine' cold grains unless the latter are present in sufficiently large quantities. This assertion is particularly apt for starburst galaxies which emit the majority of their bolometric luminosity from sites of recent star formation (Alton et al. 1998a).

NGC 5194 This almost face-on, Sbc galaxy (also known as the "Whirlpool Galaxy" and M51) has been the subject of numerous observational studies at a wide range of wavelengths (e.g. , most recently, Hill et al. 1997; Grillmair et al. 1997; Berkhuijsen et al. 1997; Sauvage et al. 1996). In particular, its grand design spiral pattern has been the testing ground for theories of spiral formation such as density wave propagation (e.g. Knapen et al. 1992). Smith (1982) has mapped NGC 5194 in a 170μm filter using the Kuiper Airborne Observatory (KAO). This study, which also included photometry at various other FIR wavelengths, showed that 70% of the energy radiated by the dust arises from the M51 disk whilst the remainder originates from NGC 5195 (the small interacting companion $4'$ to the north). In our data, the satellite is situated at the bottom right of the map and makes an obvious contribution to the recorded emission. Once again there is recognisable reciprocity between the IRAS and ISO morphology (although, note that the 'smear' in the 100μm image, towards the top-left corner of the figure, is a result of detector hysteresis in the IRAS detectors rather than any physical phenomenon). Hippelein et al. (1996) have used ISO Guaranteed Time to map M51 at wavelengths of 60, 100 and 175μm. Their longest wavelength image shows a strong resemblance to our 200μm data.

NGC 5236 This galaxy, also known as M83, is one of the closest spirals with a prominent bar (Adamson et al. 1987). At optical and near infrared wavelengths the galaxy exhibits an amorphous

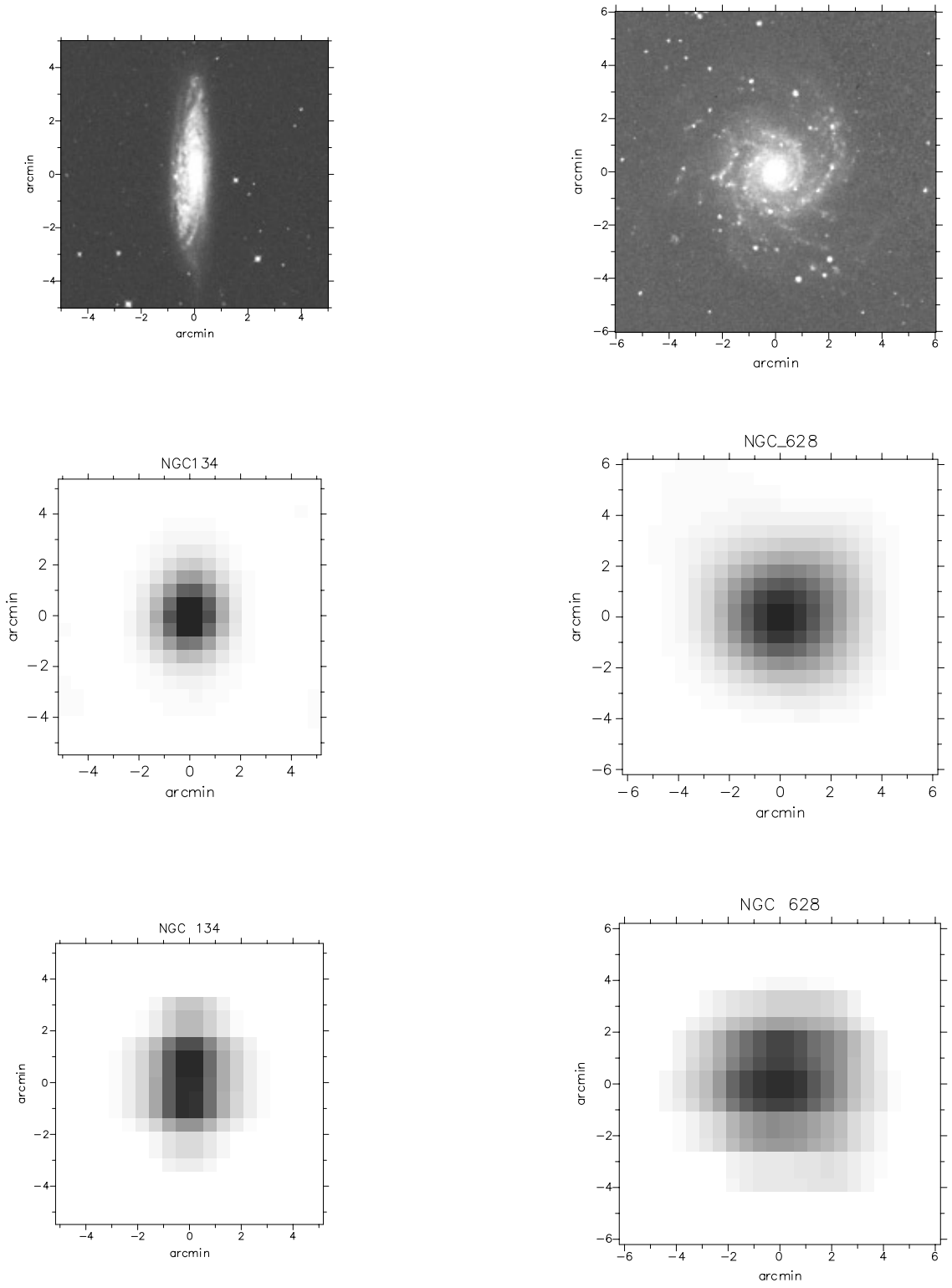

Fig. 1. Resolved 200μm images of eight nearby galaxies. In each case, the 200μm ISO data are presented as an inverse greyscale image at the bottom of the figure. The maximum surface brightness recorded at 200μm is as follows (MJy/sr): 110 (N134), 90 (N628), 200 (N660), 230 (N5194), 400 (N5236), 27 (N6822), 250 (N6946) and 220 (N7331). IRAS HiRes data, taken in a 100μm filter and smoothed to the same resolution as the ISO image, are shown as an inverse greyscale image in the middle. The maximum surface brightness at 100μm is as follows (MJy/sr): 133 (N134), 43 (N628), 367 (N660), 270 (N5194), 446 (N5236), 30 (N6822), 271 (N6946) and 210 (N7331). At the top, a B-band image shows how the corresponding galaxy appears optically (at 2$''$ resolution). The 100μm and B-band data are scaled to the same size as the 200μm image and also have the same orientation. The position angles of the ISO scans (left to right in the images) are given in Table 1.

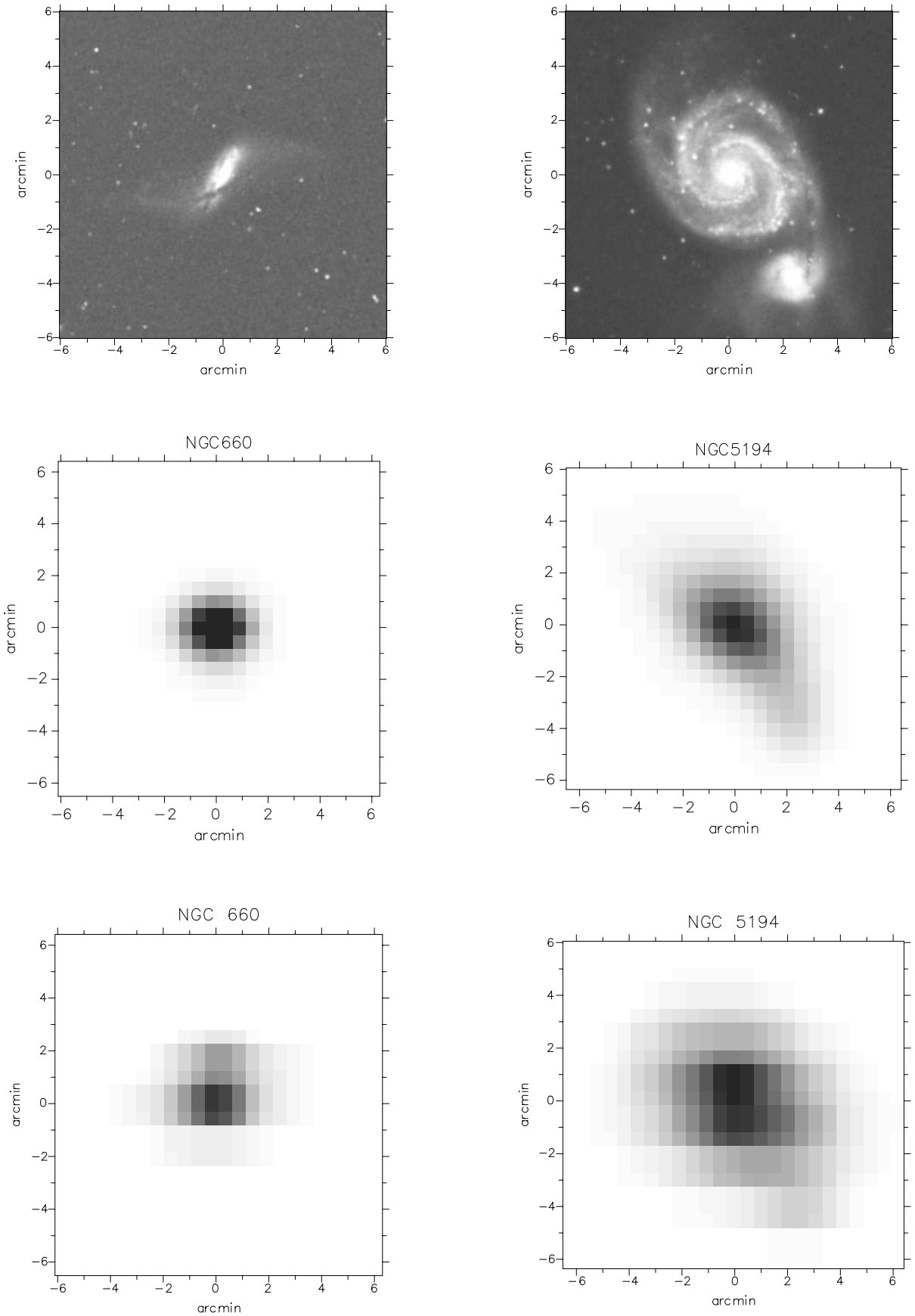

Fig. 1. (continued)

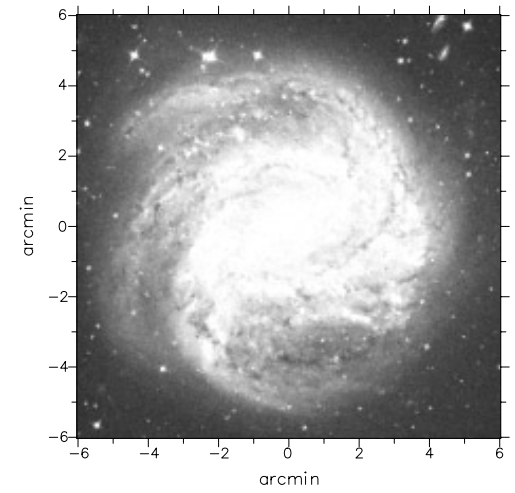

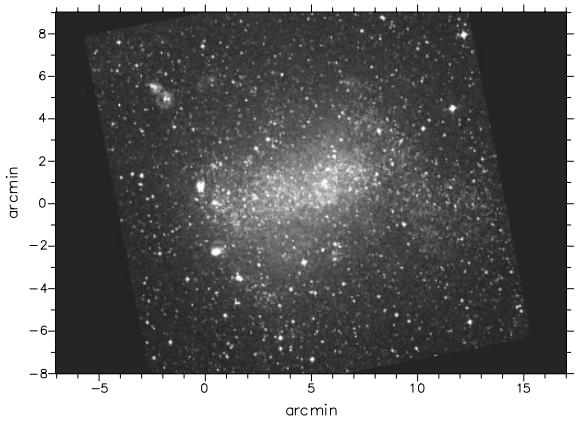

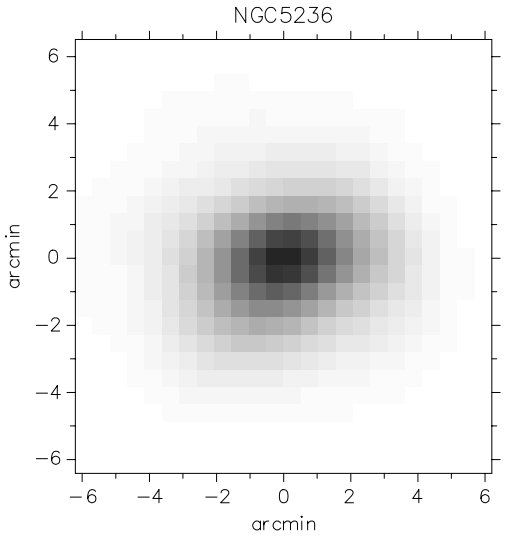

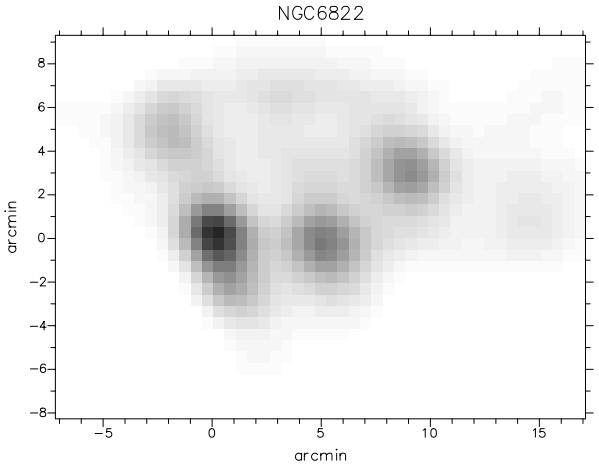

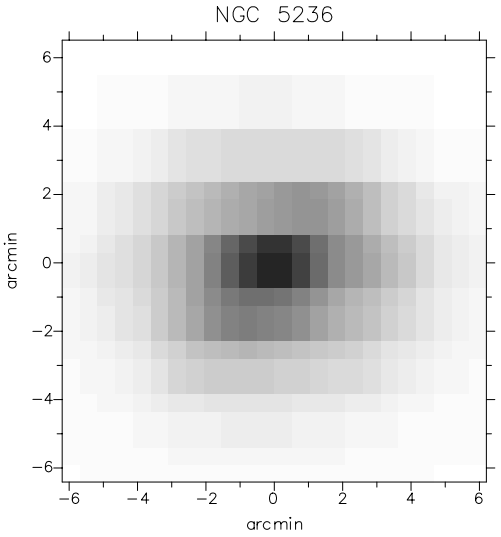

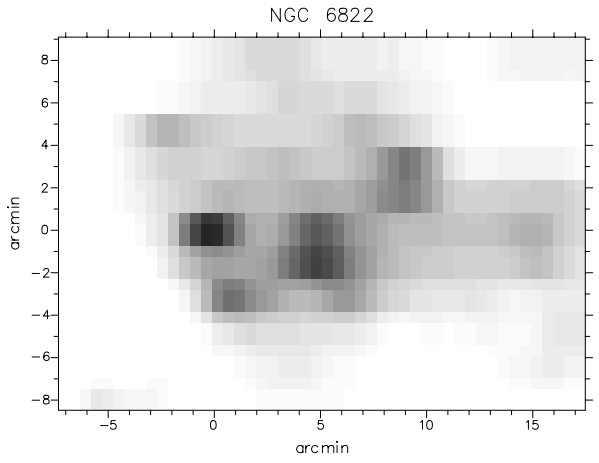

Fig. 1. (continued)

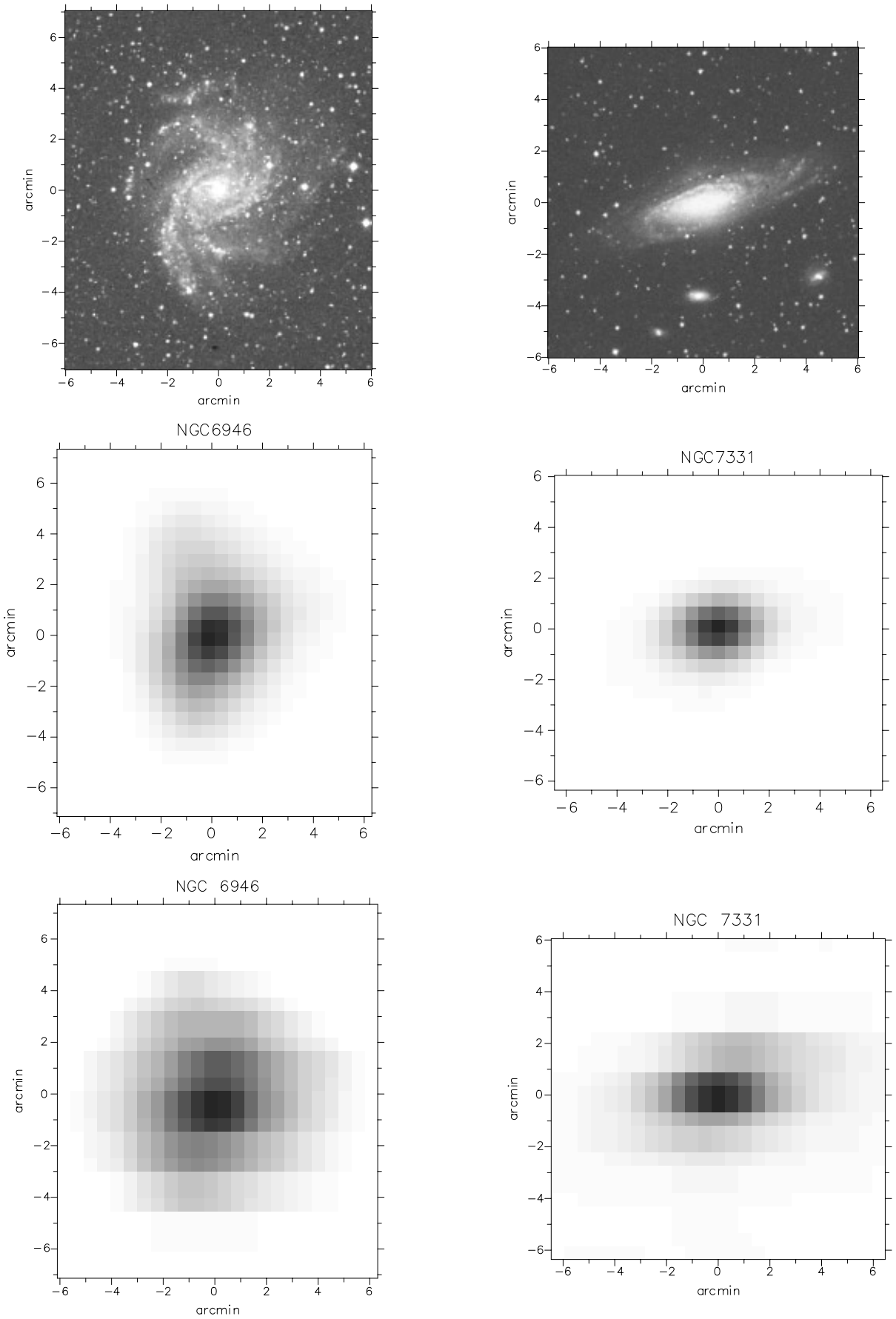

Fig. 1. (continued)

structure within the central $16''$ (Gallais et al. 1991) and this can almost certainly be associated with a mild nuclear starburst. There is bright emission in our FIR maps of M83 and some evidence for a bar structure in the 100μm image. The 200μm emission appears very extended with respect to the optical disk. Intriguingly, M83 is known to have a remarkably extensive HI disk containing 80% of its mass *outside* the optical diameter (Huchtmeier & Bohnenstengel 1981).

NGC 6822 This galaxy is something of an anomaly within our sample for it is not a large disk galaxy but in fact a dwarf irregular situated only 500kpc away within the Local Group. The galaxy's optical appearance is characterized by a non-uniform distribution of HII regions (Hodge et al. 1989) and a north-south 'bar' which comprises older stars (the latter runs left to right in Fig. 1). Israel et al. (1996), in an analysis of IRAS HiRes data for this object, concluded that only half of the FIR emission arises from discrete sources (HII regions and OB associations), the remainder probably associated with stars older than 10^7 years. The data in Fig. 1 are noteworthy because there is a fairly good spatial correspondance between the convolved 100μm data and the ISO image. Whilst this may be interesting from a physical perspective (in particular, the mechanisms by which dust is heated within *irregular* galaxies), it also reassures us that the ISOPHOT instrument can reliably resolve FIR structure within our targets.

NGC 6946 This is an Sc galaxy viewed at an inclination of about 31°. There is recent star formation throughout the spiral arm structure and a mild starburst at the centre (Tacconi & Young 1990). Our IRAS HiRes data, before convolution to the ISO 200μm resolution, appear to follow the spiral arms quite closely with maxima at the nucleus and prominent HII regions. The 200μm map in Fig. 1 exhibits a similar morphology to the 100μm data.

NGC 7331 This is a highly inclined ($i \simeq 70°$; Corradi & Capaccioli 1991) Sb galaxy with a prominent bulge which rotates retrograde with respect to the disk (Prada et al. 1996). Within the central few arcminutes there is a dearth of both atomic and molecular gas (von Linden et al. 1996). The FIR emission is already known, from KAO observations, to be rather 'flat topped' in this region (Smith & Harvey 1996). The 200μm structure resembles, to a large degree, the morphology evident in the 100μm image although the longer wavelength emission appears to be more extensive. Bianchi et al (1998a) have recently mapped NGC 7331 at 450μm and 850μm using the submillimeter array SCUBA (effective resolution of $10''$ and $15''$ respectively). They detect a bright submm ring surrounding the nucleus at a radius of 2-3 kpc. This 'dust ring' appears to be co-spatial with a concentration of molecular gas at the same radius.

4. Surface brightness profiles

The data presented in Fig. 1 provide the means to compare emission at different FIR wavelengths and also to study how dust emission relates to the distribution of stellar light. In fact, by examining the shape of the surface brightness profile at each wavelength, we can make a comparison which is independent of the absolute calibration. To do this, however, it is necessary to remove obvious stars from the B-band images in Fig. 1 and then convolve the images to the same resolution as the ISO 200μm data. After doing this, we use a standard galaxy photometry package to derive the azimuthally-averaged radial surface brightness profile at 60, 100, 200μm and in B. In general, this is achieved by fitting, along the major axis of the galaxy, photometric annuli possessing an ellipticity consistent with the optical inclination of the galaxy (thus circular annuli for a face-on galaxy). The resultant profiles are shown in Fig. 2 for all the galaxies in Table 1 except NGC 6822 (which is irregular rather than spiral). The profiles at each wavelength have been normalized to a common value at the centre so that the relative fall-off in surface brightness can be discerned. In Table 2 we also present the exponential scale-length for each waveband measured between a radius of $1.5'$ and $3.5'$.

The random errors in Fig. 2 are less than 1% (smaller than the plotted markers) but there are, nonetheless, more substantial systematic errors which would tend to flatten or steepen the curves slightly. For the B-band and IRAS curves the main source of error arises from uncertainty in the smoothing process (necessary to match their resolution to that of the ISO observations). The reason for this is that neither the IRAS nor the ISO beam is perfectly gaussian making an identical match in resolution almost impossible. For the 200μm profiles, errors are introduced from uncertainty in the sky subtraction – particularly for objects lying close to the Galactic plane. These systematic errors amount to a 4–6% uncertainty in the derived scale-lengths and are listed in Table 2.

Table 2 also shows the ratios of B-band, 60μm and 100μm scale-length with respect to the 200μm emission. The average values are 0.79 ± 0.05, 0.57 ± 0.06 and 0.56 ± 0.04 respectively. In other words the 200μm scale-length is typically 77% larger than emission detected in the IRAS wavebands and 27% larger than the scale-length of B-band light. Before discussing what implications this might have for the ISM of external galaxies, we must first be sure that our results are not an artifact of the ISOPHOT detectors or the measurement process.

5. Discussion

5.1. Instrumental checks

Whilst the determination of the surface brightness scale-lengths, carried out in the previous section, is independent of the absolute calibration of the ISO data, the shape of the ISOPHOT 200μm beam, as well as the behaviour of the detectors, must be carefully examined before attributing our profile results

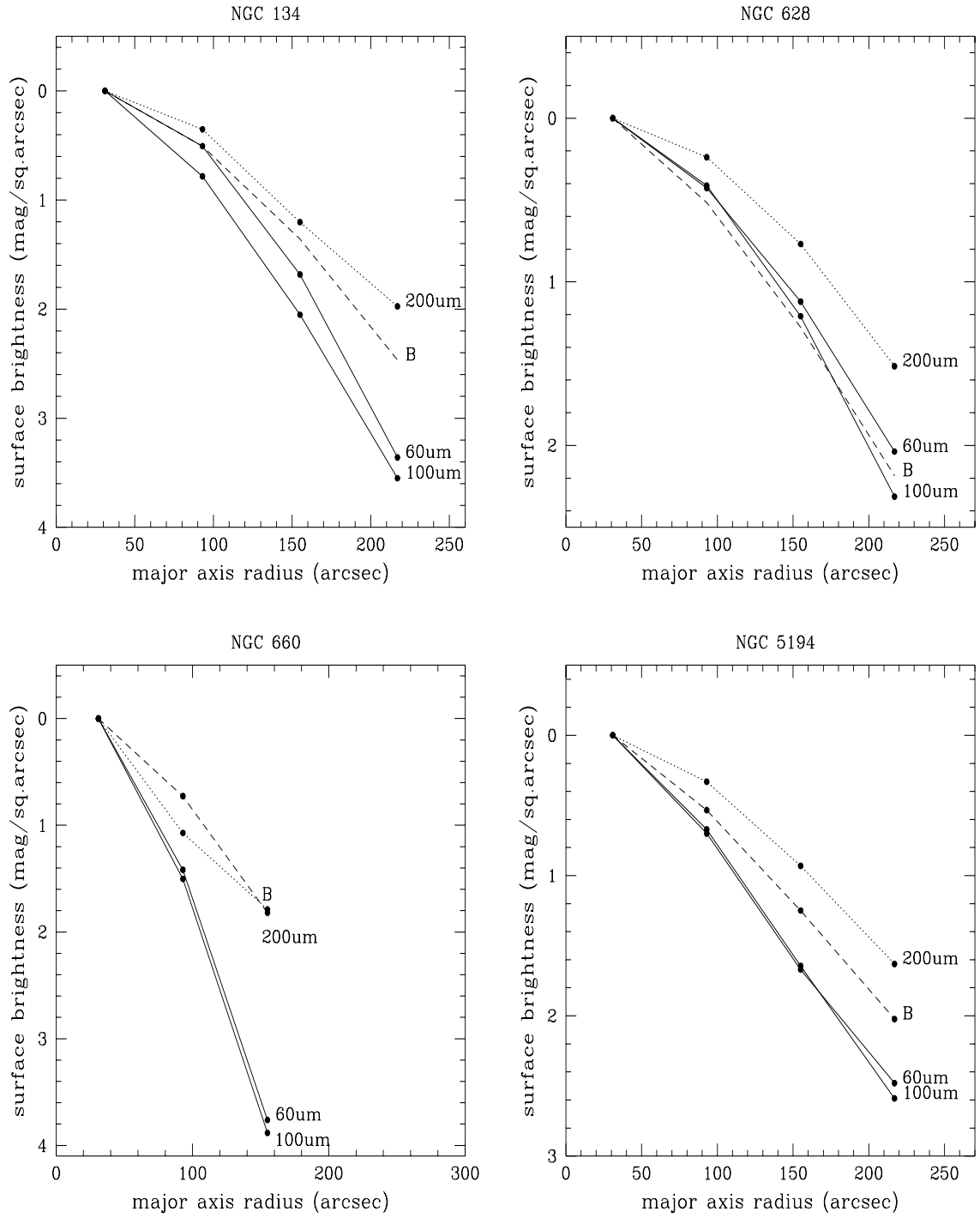

Fig. 2. Profiles of the spiral galaxies observed with ISO. The azimuthally-averaged radial surface brightness is shown for observations at 60μm and 100μm (solid lines), at 200μm (dotted line) and for the B-band filter (dashed line). The curves have been normalized to a common value near the centre in order to show the relative fall-off in surface brightness. Random errors in the data points are $<$0.01 mag which is less than the size of the plotted markers.

to physical properties of spiral galaxies. In convolving our optical and FIR data to a common resolution we have assumed a gaussian beam of 117″ (FWHM) for the 200μm data. This is the approximation given by Tuffs et al (1996) who have made a detailed analysis of ISOPHOT Performance Verification Observations. Recent observations of the point source NGC 7027, using the P32 200μm mapping mode, have been kindly made available to us by U. Herbstmeier from the Heidelberg Datacentre and these are shown in Fig. 3 along with the Tuffs et al approximation. Clearly, the 117″ gaussian we have been using provides a satisfactory approximation. If anything, it might marginally *over*-esimate the size of the ISO beam but

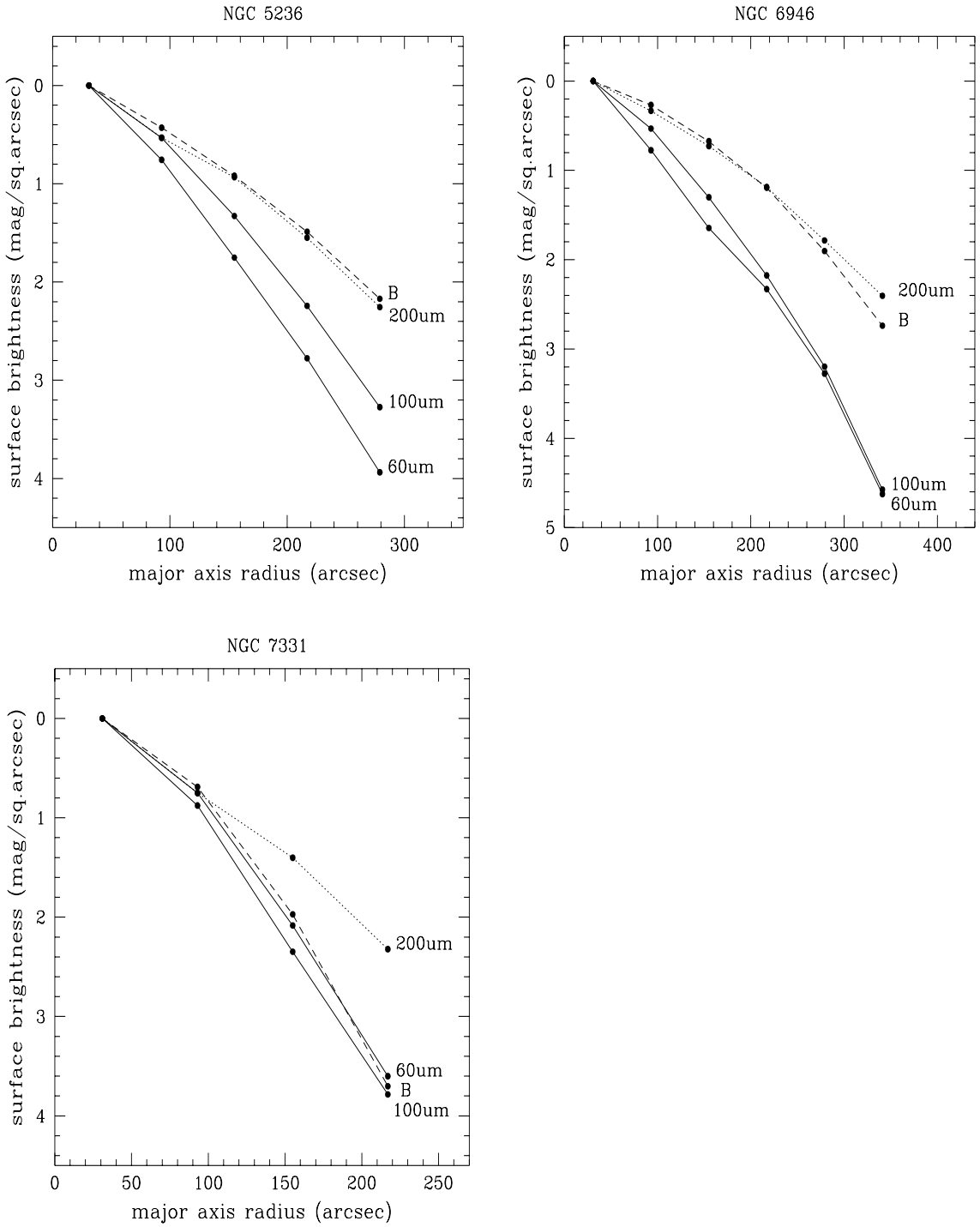

Fig. 2. (continued)

this would cause us to, if anything, *underestimate* the size of the 200μm scale-length relative to the IRAS and optical profiles.

Far infrared detectors are also susceptible to transient effects, or hysteresis, particularly after scanning bright sources such as galactic nuclei (Rice 1993). Such effects become evident as enhanced flux levels or 'stripes' in the direction of the scan. Tuffs et al (1996) have analyzed the transient behaviour of ISOPHOT but find no evidence for scanning artifacts from the C200 detectors used for the observations reported here. We, ourselves, undertook 2 checks on the same problem. Firstly, we repeated the profiling carried out in the previous section but, on this occasion, divided the galaxy into 4 quadrants so that the scale-length could be derived for both the *in-scan* direction and the *cross-scan* direction. We have found that profiling with just the cross-scan data alters our conclusions only slightly. For

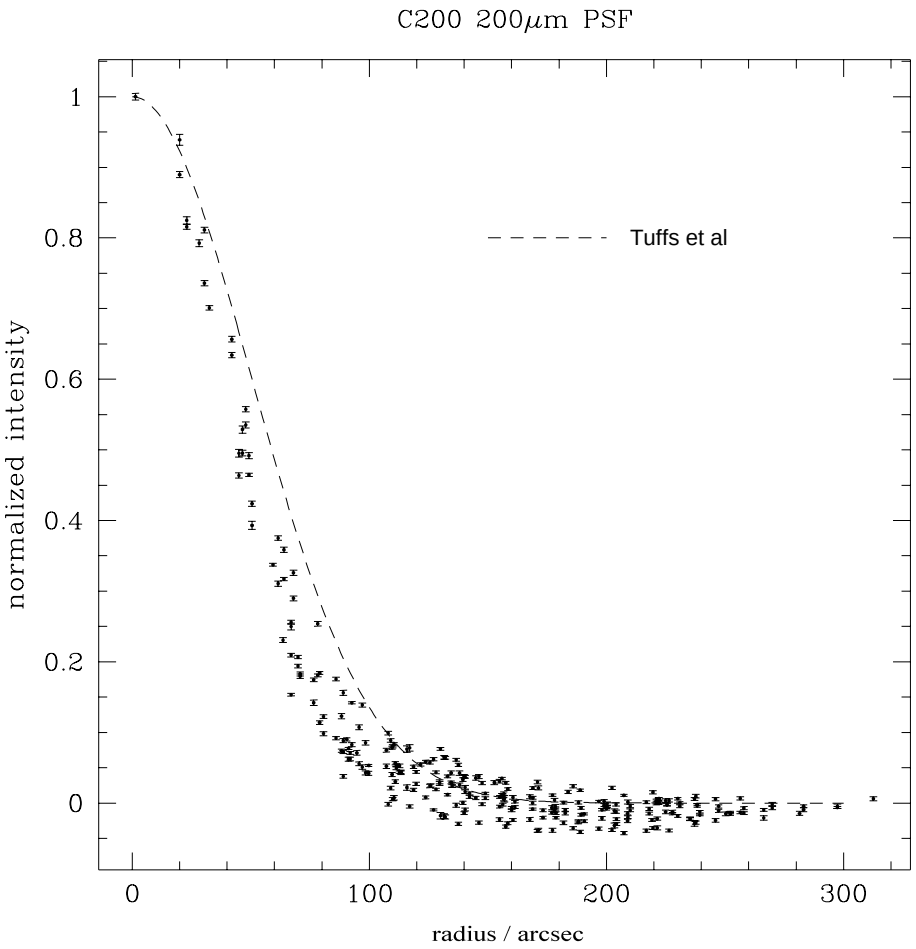

Fig. 3. Mapping measurements of the point source NGC 7027 taken in the ISOPHOT 200μm filter. The markers denote the relative intensity against radial distance from the central position. The dashed line shows the gaussian approximation (FWHM $\simeq 117''$) used by the ISOPHOT instrument team to describe the 200μm beam (Tuffs et al (1996)).

example, we obtain a mean 100μm-to-200μm ratio of 0.61 instead of a value of 0.57 derived from the scale-lengths in Table 2.

The second check came from examining the 200μm data for NGC 660. In distinct contrast to all the other spirals in our sample, NGC 660 is characterized by a high FIR-to-blue luminosity ratio indicative of prolific recent star formation (Alton et al 1998a). In both the 60μm and 100μm IRAS filters the emission is unresolved, arising essentially from an energetic starburst located within the central 3 kpc of the galaxy. At 200μm the emission is basically compact but some faint, extended structure is also apparent (Fig. 1). Whilst some of this extended structure may well be associated with emission from the outer disk and polar ring (orientated roughly left-to-right in Fig. 1), we will assume for the sake of argument that it arises purely from a transient behaviour in the detectors after scanning the bright nucleus (the scan direction is also from left to right). Assuming this "worst case scenario" we assess how this might undermine our results. The width of the NGC 660 200μm emission, for the in-scan direction, is measured to be $\simeq 150''$ (FWHM) which is slightly broader than the ISO beamwidth of $117''$. We took, therefore, the IRAS 60μm and 100μm images for our galaxy sample and smoothed them to a resolution of $150''$ (instead of the $117''$ used previously). After re-profiling the convolved images we noted that the effect of this treatment was to decrease the 200μm-to-60μm and 200μm-to-100μm scale-length ratios by about 10%. This small difference is *not* enough to account for the fact that the 200μm scale-length appears to be $\sim$ 80% longer than the scale-length in the IRAS filters.

Curiously, Tuffs et al (1996), who have mapped one of our objects (NGC 6946) at both 60μm and 200μm, find an almost constant ratio at these two wavelengths with radius. The observations in question were carried out with ISO during the Performance Verification phase of the mission using the C100 detector with the 60μm filter and the C200 detector at 200μm. The discrepancy with our own results seems to arise from the 60μm measurement. For the Tuffs et al data, the 60μm scalelength is measured to be $191''$ (Lu et al 1996) whereas we record a value of $87''$ using IRAS HiRes data (Table 2). The difference could be connected with an apparent susceptibility of the ISO C100 detector to transient memory effects (Lemke et al. 1996). Indeed, Tuffs et al admit that there is a factor of 2 change in the 60μm/200μm scalelength ratio for the cross-scan photometry compared with that in the in-scan direction (a possible symptom of detector hysteresis). To substantiate this claim we have compared our data for NGC 6946 with KAO observations of the same galaxy. Engargiola (1991) has analysed 60μm and 100μm images

of N6946 taken with IRAS (HiRes) and KAO respectively. For these two wavelengths he derives scalelengths of $60''$ and $78''$ respectively. The proximity of these values to those appearing in Table 2 suggest a good agreement between KAO and IRAS. (Furthermore, the total fluxes at 60μm and 100μm measured by KAO, are within 10% of the corresponding values measured by IRAS for 7 nearby galaxies including NGC 6946 (Engargiola 1991 – Table 1C)). We suggest that the scalelengths derived from ISO C100 data (such as those in Tuffs et al) may overestimate their true values by a factor of 2.

After carrying out the careful checks described above, we concluded that the broader emission we detect at 200μm is a physical property of spiral galaxies rather than an artifact of the measurement process.

5.2. Physical implications

A broadening of the radial profile for longer FIR wavelengths implies colder dust at larger radii. This result is consistent with the findings of Engargiola (1991) and Smith (1982) both of whom observed objects in Table 1 using KAO. Smith (1982) observed M51 in 55, 130, 170, 320 μm filters and found a drop in dust temperature between the nucleus (20 K; β=2) and the outer disk (17 K; β=2). Engargiola (1991) has mapped the whole of NGC 6946 at 160μm and also the central $5'$ region in a 200μm filter. Availing himself of the HiRes IRAS data for this object, he found an increase of 40% in the scale-length at 200μm compared to the scale-lengths measured at 60μm and 100μm. Although we find an increase of about 85% from our own data (Table 1), the 200μm observations carried out by Engargiola do not extend as far out, radially, as our own measurements. Moreover, at the periphery of the $5'$ region mapped by Engargiola there is a strong indication that the scale-length at 200μm becomes much larger, in line with our own observations (see Fig. 3b in Engargiola (1991)). It is also noted that edge-on galaxies which have been mapped at IRAM, manifest a 1.2mm (1.3mm) major axis profile which is significantly broader than emission at shorter wavelengths (Guelin et al 1993; Neininger et al 1996). Again this is a clear indication that cold dust becomes more prevalent towards the optical edge of spiral disks.

Another corollary to the profiles shown in Fig. 2 is that the 200μm emission has a similar scale-length to that of the B-band light. Given that the warmest grain temperatures are found at the centre of the galaxy, where the interstellar radiation field is the most intense, the dust surface density must actually be broader than the 200μm emission profile. This indicates that the dust is more radially extended than the stars (the latter being traced, in some measure, by the blue light). This inference is in accordance with photometric modelling of edge-on spiral galaxies where the dust layer is generally found to have a radial scale-length 50% larger than that of the stars (Xilouris et al (1997a,b); Kylafis & Bahcall 1987).

Cold dust at larger galactic radii immediately has two major implications for the ISM of spiral disks: (1) Dust emitting primarily at 200μm may be heated by a different radiation source than the warmer grains detected by IRAS; and (2) Spiral disks may harbour far larger quantities of interstellar dust than has been hitherto surmised from IRAS data. It is tempting to (re)assert that IRAS is sensitive to warm dust associated with HII regions. This argument has already been advanced by Devereux et al (1995,1997) who find a convincing spatial correlation between $H\alpha$ flux and 60μm (100μm) emission in nearby spirals. Furthermore, the fact that, for nearby galaxies, the ratio of 60μm-to-100μm emission appears to be constant with radius (Devereux & Young 1993; see also the profiles in Fig. 2), might indicate that both the 60μm and 100μm IRAS filters sample the same dust environment (HII regions, OB associations) regardless of galactic radius. In contrast, it seems likely that the 200μm emission, detected by ISO, is more sensitive to dust bathed in the general interstellar radiation field where lower grain temperatures are expected to prevail.

As we have both IRAS and ISO calibrated data we can make a quantitative measurement of how the ISO flux affects the determination of dust temperature and mass. Although, in practice, intersellar grains must possess a range of temperatures the simplest procedure is to assume that the data can be fitted by a single blackbody curve modified by a power law emissivity of index β. Intriguingly, there is no single curve that provides a good fit to both the IRAS 60μm and 100μm points and the ISO 200μm flux (and, unfortunately, we have an insufficient number of data to fit for both a warm and a cold dust component simultaneously). We can, however, fit to the two IRAS points and then to the IRAS 100μm and ISO 200μm points. This will indicate how the ISO data alter our perceptions of dust mass and temperature. These estimates may, in turn, need to be remodified once dependable submm observations become available, although existing measurements indicate that the major dust mass component has a temperature of about 20 K (Chini 1996). We also emphasize that thermally-spiked grains (size $<$ 100Å), which are not in equilibrium with the surrounding radiation field, are likely to contribute significantly to the flux detected in the IRAS 60μm filter ($\sim$ 50%; Désert et al (1990); Draine & Anderson (1985)). Since our intention at this stage, however, is to show how our inferences might have to change with the advent of new, longer wavelength data, we simply follow the same 'recipe' for fitting IRAS 60μm and 100μm data that has been adopted in the past.

For each of the objects in Table 2, we have derived the total flux within a 1σ isophote at 60, 100 and 200 microns. These data are shown in Table 3. We have then applied greybody fits (β=1 and β=2) to: (1) the integrated IRAS (60μm & 100μm) values and (2) the ISO (100μm & 200μm) values. In addition, by adopting the far infrared emissivity given by Hildebrand (1983),

and using the distances listed in Table 1, we were able to derive the total dust masses. Thus:

$$M_d = \frac{4a\rho D^2}{3}\frac{F_\nu}{Q_\nu B_{\nu,T}} \quad (1)$$

where M_d, D, a and ρ are the dust mass, galaxy distance, grain radius and grain material density respectively. F_ν, Q_ν and $B_{\nu,T}$ are the observed flux density, the grain emissivity and the value of the Planck function at the frequency ν. For the grain parameters we use the classical grain values given by Hildebrand. Thus $a = 0.1\mu$m, $\rho = 3000$kgm^{-3} and:

$$Q_\nu = \frac{3}{4000}\Big(\frac{\nu}{\nu_{125\mu m}}\Big) \quad (2)$$

or

$$Q_\nu = \frac{3}{1300}\Big(\frac{\nu}{\nu_{125\mu m}}\Big)^2 \quad (3)$$

depending on whether a power index of 1 or 2 is adopted for the FIR emissivity law. Table 4 shows the mean dust properties obtained from the greybody fitting procedure and the dust mass calculations. Although there is some uncertainty in the FIR emissivity, the *ratio* of IRAS-to-ISO dust mass is reasonably secure.

It is clear that, by using IRAS data alone, we underestimate the amount of dust present by an order of magnitude and overestimate the grain temperature by about 10 K. In fact, the simple greybody fitting technique we have employed is likely to underestimate the difference in temperature between the warm dust and the main cool dust component. This is because, in deriving the temperature for the ISO data, we have used the same 100μm flux that we used in order to derive the IRAS temperature. Since the 100μm filter is already likely to contain a strong contribution from warm dust, any temperature we derive for the cold component is likely to be an overestimate. In other words, to account for the 200μm emission detected by ISO, substantial quantities of dust colder than 18-21 K must be present.

Using HI and H_2 data presented in Devereux & Young (1990), we have derived average gas-to-dust ratios based on IRAS and ISO data respectively. Estimates based on the latter (Table 4) are clearly more in line with what we measure for the ISM of our own Galaxy (Gas-to-dust ratio=150–300; Whittet 1992), suggesting that as we observe spirals at longer wavelengths we obtain a more realistic picture of their dust content. As noted in Sect. 2.1, it is possible that the present photometric calibration of ISOPHOT data overestimates the 200μm flux by $\sim 30\%$. Table 4, therefore, gives an indication of how our perceptions of dust mass and temperature would change assuming the 200μm integrated fluxes are, in fact, only 70% of their recorded values. Once again, we expect nearly an order of magnitude more dust to be present than if we had simply used IRAS data.

Apart from the implications for the amount of dust in external spiral disks, our results have interesting ramifications for the nature of the ISM and the overall disk opacity. Since the 200μm scale-length is slightly larger than the B-band scale-length, there is a strong indication that the cool dust is radially more extensive than the stellar disk. Notably, if this dust layer were optically thick, the increased extinction towards the galaxy centre would act to flatten the distribution of blue light leading to a B-band scale-length much larger than that of the 200μm emission. We have tested this idea by running Monte Carlo radiative transfer models of spiral disks possessing exponential distributions of dust and stars (Bianchi et al 1998b). Only if the dust gradient is 2-3 times *less* steep than that of the stellar disk, can we reproduce the observed ratio of B-band-to-200μm scale-lengths. Moreover, the putative dust layer must be optically thin. Such a scenario seems irreconcilable with the fact that normal spirals emit approximately half of their bolometric luminosity in the FIR (Soifer et al 1987) – a testament to significant optical depth over at least some parts of their disk. To account for this 'dust-reprocessed' energy we require a second grain component which is optically thick. Thus, we favour a scenario in which, in addition to an optically thin, radially-extensive, cool dust component, there exists a clumpy, optically-thick medium probably associated with the dense gas enshrouding sites of recent star formation. The latter component contains warm grains which give rise to the majority of the FIR emission.

Is it possible that the extended disk of cold dust we have detected using ISO is associated with the broad HI disks known to exist in many spiral galaxies ? Several of the galaxies in our sample are characterized by a diffuse envelope of atomic gas which stretches significantly beyond the optical disk (e.g. NGC 6946 and M51; Tacconi & Young 1986, Rots et al. 1990). In a few extreme cases the majority of HI is found at several times beyond the optical radius (e.g. NGC 5236 and NGC 628; Huchtmeier & Bohnenstengel 1981, Briggs et al. 1980). For the galaxies NGC 6946 and M51, we have tried to gauge whether the faint HI envelope can be reasonably associated with the 200μm emission we record beyond the optical disk. To do this, we have assumed a Galactic extinction law and a solar gas-to-dust ratio. NGC 6946 possesses a HI column density of 6.8×10^{20} atoms cm^{-2} at the optical radius, R_{25}. Thus, we use the relation given by Bohlin et al (1978), which connects reddening in the Galaxy with mean gas column density, to derive a V-band optical depth of 0.32 for the outer regions of NGC 6946. Next we predict the 200μm surface brightness corresponding to this optical depth, using the mean grain properties in Table 4 (β=1, T=21 K; β=2, T=18 K). Assuming an extinction efficiency, σ_{ext} of 1.5 (Whittet 1992), and using once again the FIR emissivity given by Hildebrand (1983), we anticipate about 18 MJy/sr at the optical edge of NGC 6946. From our ISO image we measure 35 ± 11 MJy/sr. Given the inherent uncertainties in the calculation, in particular the sensitivity of luminosity on temperature ($T^{5\rightarrow6}$) and our ignorance of the true FIR emissivity, the agreement is surprisingly good. In fact, the same calculation for the outer climes of M51

(N_H = 3×10^{20} atoms cm^{-2}; Rots et al (1990)) also leads to a surprisingly good agreement. Certainly if our temperature for the cold grains is approximately correct (18–21 K), we appear to be detecting enough 200μm flux to account for emission from a broad HI envelope.

6. Conclusions

We have recently obtained 200μm images of 8 nearby galaxies using the ISOPHOT instrument onboard the Infrared Space Observatory (ISO). All the objects observed, with the exception of one, are nearby spirals which have been selected because their angular sizes ($D_{25} \sim 10'$) optimize the resolution of the ISOPHOT instrument (FWHM $\simeq$ 117″). We also obtained 60μm and 100μm IRAS data (resolution $\sim$ 1′) and B-band images for our galaxy sample. After convolving the optical and FIR data to a common resolution, and making careful checks on the behaviour of the ISO detectors and beam profile, we found that the exponential scale-length at 200μm is about 80% longer than that of the IRAS bands and comparable to that of the B-band. We infer from this that; (1) cold dust becomes more prevalent at larger radii and (2) these cold grains are more radially extended than the stars (the latter traced, in some measure, by the blue light).

It is tempting to claim that IRAS is sensitive primarily to warm dust from HII regions whereas ISO detects emission from grains heated by the general interstellar radiation field. Gas-to-dust ratios of external spirals, derived on the basis of IRAS data, have always been considered enigmatically high compared to the Galaxy (Devereux & Young 1991). We have tested, therefore, how the new ISO measurements change our perceptions of dust mass and temperature within external disks. Blackbody fits to the 100μm and 200μm data, modified by a $\beta = 1 \rightarrow 2$ emissivity law, give grain temperatures 10 K less, and dust masses an order of magnitude higher, than the corresponding fits to the IRAS data alone (60μm and 100μm). These revised values are consistent with a solar gas-to-dust ratio and heating by the general interstellar radiation field (we derive $T \leq$ 18-21 K).

By including 200μm fluxes, we find that the peak in the far infrared spectral energy distribution (SED) lies at $\simeq 170\mu$m i.e. well beyond the longest wavelengths observed by IRAS. The ISO observations allow us, therefore, to sample most of the FIR energy emitted by interstellar dust grains. By collating optical and near infrared (NIR) images for our galaxy sample it will be possible to study the dust heating mechanisms in spiral disks and, more generally, the overall energy budget. A comparison of the SED in the optical/NIR regime with that measured in the FIR, will indicate the level of extinction taking place in spiral disks (Trewhella 1997; Trewhella et al 1998).

Acknowledgements. We are grateful to members of the ISOPHOT instrument team for assistance in processing the ISO observations. In particular, we are indebted to Phil Richards at RAL and Carlos Gabriel at Vilspa for useful discussions on the PIA software. U.Herbstmeier and the staff of Heidelberg Datenzentrum are acknowledged for making measurements of the ISO beam available to us. We also thank the staff at IPAC for supplying us with IRAS HiRes images of our galaxies. PBA is supported by a PPARC grant.

References

Adamson, A.J., Adams, D.J. & Warwick, R.S., 1987, MNRAS, 224, 367
Alton, P.B., 1996, Ph.D., University of Durham
Alton, P.B., Davies, J.I., Trewhella, M., 1998a, MNRAS in press
Alton, P., Bianchi, S., Rand, R., Davies, J., Xilouris, E., 1998b, MNRAS in prep
Armus, L., Heckman, T.M., Miley, G.K., 1990, ApJ, 364, 471
Aumann, H.H., Fowler, J.W. & Melnyk, M., 1990, AJ, 99, 1674
Bianchi, S., Alton, P., Davies, J., Trewhella, M., 1998a, MNRAS submitted
Bianchi, S., Davies, J.I., Alton, P.B., Trewhella, M., 1998b, MNRAS in prep
Block, D., 1996, in 'New Extragalactic Perspectives in the New South Africa', Kluwer, ed. D.Block and J.Mayo Greenberg
Bosma, A., Byun, Y., Freeman, K., Athanassoula, E., 1992, ApJ, 400, L21
Briggs, F.H., Wolfe, A.M., Krumm, N., Salpeter, E.E., 1980, ApJ, 238, 510
Cepa, J. & Beckman, J., 1990, ApJ, 349, 497
Chini, R., 1996, in 'New Extragalactic Perspectives in the New South Africa', Kluwer, ed. D.Block and J.Mayo Greenberg
Condon, J.J., Helou, G., Saunders, D.B., Soifer, B.T., 1996, ApJS, 103, 81
Corradi, R.L.M. & Capaccioli, M., 1991, A&AS, 90, 121
Davies, J.I. & Burstein, D., 1995, in 'The opacity of Spiral Disks', proceedings of NATO ARW, NATO Asi Ser. 469, ed. J.Davies and D.Burstein
Davies, J.I., Phillipps, S., Trewhella, M., Alton, P.B., 1997b, MNRAS in press
Désert, F., Boulanger, F., Puget, J., 1990, A&A, 237, 215
Devereux, N.A. & Young, J.S., 1990, ApJ, 359, 42
Devereux, N. & Young, J., 1993, AJ, 106, 948
Devereux, N., Jacoby, G., Ciardullo, R., 1995, AJ, 110, 1115
Devereux, N., Duric, N., Scowen, P., 1997, AJ, 113, 236
Disney, M.J., Davies, J.I. & Phillips, S., 1989, MNRAS, 239, 939
Bohlin, R., Savage, B., Drake, J., 1978, ApJ, 224, 132
Draine, B. & Lee, H., 1984, ApJ, 285, 89
Draine, B., Anderson, N., ApJ, 292, 494
van Driel, W., de Graauw, Th., de Jong, T., Wesselius, P.R., 1993, A&A, 101, 207
van Driel, W., Combes, F., Casoli, F. et al, 1995, AJ, 109, 942
Engargiola, G., 1991, ApJS, 76, 875
Evans, Rh, 1992, Ph.D. University of Wales Cardiff
Gallagher, J.S., Hunter, D.S., Gillet, F.C. & Rice, W.L., 1991, ApJ, 371, 142
Gallais, P., Rouan, D., Lacombe, F., Tiphene, D., Vauglin, I., 1991, A&A, 243, 309
Grillmair, C.J., Faber, S.M., Lauer, T.R. et al 1997, AJ, 113, 225
Guelin, M, Zylka, R., Mezger, P., Haslam, C., Kreysa, E., Lemke, R., Sievers, A., 1993, A&A 279, L37
Guelin, M., Zylka, R., Mezger, P., Haslam, C., Kreysa, E., 1995, A&A 298, L29
Hauser, M., Silverberg, R., Stier, M., Kelsall, T., Gezari, D., Dwek, E., Walser, D., Mather, J., Cheung, L., 1984, ApJ, 285, 74

Hildebrand, 1983, QJRAS, 24, 267
Hill, J.K., Waller, W.H., Cornett, R.H. et al, 1997, ApJ, 477, 673
Hippelein, H., Lemke, D., Tuffs, R.J. et al, 1996, A&A, 315, L79
Hodge, P.W., Lee, M.G., Kennicutt, R.C., 1989, PASP, 101, 32
Huchtmeier, W.K. & Bohnenstengel, H.D., 1981, A&A, 100,72
Israel, F.P., Bontekoe, T.R., Kester, D.J.M., 1996, A&A, 308, 723
Kennicutt, R.C. & Hodge, P.W., 1980, ApJ, 2411, 573
Kessler, M., Steinz, J.A., Anderegg, M.E. et al, 1996, A&A, 315, L27
Knapen, J.H., Beckman, J.E., Cepa, J., van der Hulst, T., Rand, R.J., 1992, ApJ, 385, L37
Kylafis, N. & Bahcall, J., 1987, ApJ, 317, 637
Lemke, D., Klaas, U., Abolins, J. et al, 1996, A&A, 315, L64
von Linden, S., Reuter, H.P., Heidt, J., Wielebinski, R., Pohl, M., 1996, A&A, 315, 52
Lu, N., Helou, G., Tuffs, R., Xu, C., Malhotra, S., Werner, M., Thronson, H., 1996, A&A 315, L153
Masi, S., Aquilini, E., Boscaleri, A., de Bernadis, P., de Petris, M., Natale, V., Palumbo, P., Scaramuzzi, F., 1995, ApJ, 452, 253
Mathis, J., Mezger P., Panagia, N., 1983, A&A, 128, 212
Neininger, N., Guelin, M., Garcia-Burillo, S., Zylka, R., Wielebinski, R., 1996, A&A 310, 725
Prada, F., Gutierrez, C.M., Peletier, R.F., McKeith, C.D., 1996, ApJ, 463, L9
Reach, W., Dwek, E., Fixsen, D., et al., 1995, ApJ, 451, 188
Rots, A., Bosma, A., van der Hulst, J., Athanassoula, E., Crane, P., 1990, AJ, 100, 387
Rice, W., 1993, AJ, 105, 67
Sandage, A. & Tammann, G.A., 1981, *A Revised Shapley-Ames Catalog of Bright Galaxies*, Carnegie Institute of Washington Publication
Sauvage, M., Blommaert, J., Boulanger, F. et al, 1996, A&A, 315, L89
Shostak, G.S. & van der Kruit, P.C., 1984, A&A, 132, 20
Smith, B.J. & Harvey, P.M., 1996, ApJ, 468, 139
Smith, J., 1982, ApJ, 261, 463
Soifer, B.T., Sanders, D.B., Madore, B.F. et al 1987, ApJ, 320, 238
Tacconi, L. & Young, J., 1986, ApJ, 308, 600
Tacconi, L.J. & Young, J.S., 1990, ApJ, 352, 595
Trewhella, M., 1997, PhD Thesis University of Wales
Trewhella, M., Davies, J., Alton, P., Bianchi, S., 1998, MNRAS in prep.
Tuffs, R.J., Lemke, D., Xu, C. et al, 1996, A&A, 315, L149
Valentijn, E., 1990, Nature, 346, 153
Vila-Costas, M.B. & Edmunds, M.G., 1992, MNRAS, 259, 121
Whittet, D., 1992, *Dust in the Galactic Environment*, IOP Publishing
Xilouris, E., Kylafis, N, Papamastorakis, J., Paleologou, E., Haerendel, G., 1997, A&A, 325, 135
Xilouris, E., Alton, P., Kylafis, N., Trewhella, M., Davies, J., Papamastorakis, J., 1998, A&A, 331, 894
Xu, C., Helou, G., 1996, ApJ 456, 163